J Mater Sci (2007) 42:1393–1396
DOI 10.1007/s10853-006-1312-0

LETTER

Effect of unidirectional drawing process on fracture behavior of poly(L-lactide)

Mitsugu Todo

Received: 20 November 2006 / Accepted: 22 November 2006 / Published online: 23 January 2007

Poly(L-lactide) (PLLA) has widely been used as a polymeric biomaterial mainly owing to its bioabsorbability and biocompatibility. For example, PLLA has successfully been used for bone fixation devices in oral and orthopedic surgeries [1]. Although application of PLLA medical devices is rapidly growing, the deformation and fracture behavior of PLLA has not fully been understood yet. Fundamental mechanical properties of thin PLLA films have already been evaluated [2–5]; however, few studies have performed to understand such properties of bulk sheet samples. Recently, Todo et al. have extensively investigated the fracture properties and behavior of PLLA plate specimens [6–11], and clarified the effects of annealing, crystallization, hydrolysis and loading-rate on the fracture behavior. Drawing process is known to be an effective way to improve the mechanical properties of thermoplastics, and effects of drawing on tensile and fracture properties of thermoplastics have been studied [12–16]. PLLA is usually draw-processed when it is used for bone fixation devices, and therefore, fundamental effect of drawing on its fracture behavior needs to be characterized.

In the present study, plate samples of amorphous PLLA were prepared, and draw-processed unidirectionally at different draw ratios. Critical J-integral at crack initiation, J_{in}, was evaluated as a mode I fracture property in the directions perpendicular and parallel to the drawing direction, i.e. the direction of molecular orientation. Scanning electron microscopy (SEM) of fracture surfaces was also performed to characterize the effects of drawing on the fracture micromechanism. The roughness of these fracture surfaces were also measured using a laser microscope to assess the relationship between the surface roughness and the fracture properties, and tried to be correlated with the fracture micromechanism.

PLLA pellets (Lacty#5000, Shimazu Co. Ltd.) were used to fabricate plates of $160 \times 160 \times 5$ mm^3 using a hot press under a processing condition of 180 °C, 30 MPa and 30 min, and then, quenched using ice water at 0 °C for 10 min to obtain amorphous state. The PLLA plates were then draw-processed using a unidirectional drawing machine at a displacement speed of 150 mm/min at 120 °C. The draw ratio was varied from 1 to 2.5. Single-edge-notch-bend (SENB) specimens were prepared from these plates, and the initial notches were introduced in the direction perpendicular or parallel to the drawing direction. It is noted that the thicknesses of the specimens were varied from 5 mm for the non-drawing original specimens to 2.2 mm for the draw-processed specimens with draw ratio of 2.5. The two different types of the draw-processed specimens were thereafter denoted as 'perpendicular' and 'parallel' corresponding to their notch directions to the draw direction. Thus, cracks were supposed to propagate in the directions perpendicular and parallel to the drawing direction in the 'perpendicular' and the 'parallel' specimens, respectively.

Three-point bend tests of the SENB specimens were performed at a quasi-static rate of 1 mm/min using a servohydraulic testing system with use of a digital recorder for measurement of time histories of load, P,

M. Todo (✉)
Research Institute for Applied Mechanics,
Kyushu University, 6-1 Kasuga-koen, Kasuga,
Fukuoka 816-8580, Japan
e-mail: todo@riam.kyushu-u.ac.jp

and displacement, δ. From each of the P–δ relations, the critical energy, U_{in}, at crack initiation was evaluated by numerically integrating the curve up to the critical point at which initiation of crack growth took place. The critical point in P–δ relation was defined as the point where rapid decrease of the specimen stiffness $dP/d\delta$ occurred. The critical J-integral at crack initiation, J_{in}, was evaluated using the following formula:

$$J_{in} = \frac{\eta U_{in}}{B(W-a)} \tag{1}$$

where B, W, and a are the thickness, width and initial crack length of the specimen. The geometrical correction factor η is 2 for the standard SENB specimen.

The average roughness values, R_a, of fracture surfaces in the crack initiation regions of the SENB specimens were measured using a laser microscope with surface profile measurement system. For each specimen, laser scanning was conducted along a line of 250 μm in length distant from the crack-tip by 50 μm. R_a is defined as the average value of the absolute values of height and depth measured from the level line, and given by

$$R_a = \frac{1}{l}\int_0^l |f(x)|\, dx \tag{2}$$

where $f(x)$ is the surface profile curve expressing roughness, and l the length of the scanning line (250 μm). Fracture surfaces were also observed to visualize the surface roughness using a scanning electron microscope (SEM). The SEM microphotographs were also utilized to characterize fracture micromechanisms.

At maximum load point, loading to a SENB specimen stopped, and unloaded to obtain an arrested crack with damage zone formed in the vicinity of the crack. A small portion containing the arrested crack was cut off from the specimen, and then a thin section was prepared on a slide glass introducing the petrographic thin sectioning technique [17, 18]. These thin samples were then observed using a polarizing optical microscope (POM) to characterize crack growth behavior.

Dependence of draw ratio on J_{in} is shown in Fig. 1. For the parallel, J_{in} decreased with increase of draw ratio, and J_{in} for draw ratio of 2.5 became about one fifth of the original. On the contrary, for the perpendicular, J_{in} increased as draw ratio increased, and J_{in} for draw ratio of 2.5 became five times greater than that of the original. Thus, greater energy is needed for crack propagation in the perpendicular than in the parallel. This is easily understood by considering the effect of drawing on the micromechanism of fracture. In draw-processed polymer, molecules are reoriented in the drawing direction. Therefore, energy dissipation during crack growth by elongation and scission of such oriented molecules is much greater in the perpendicular

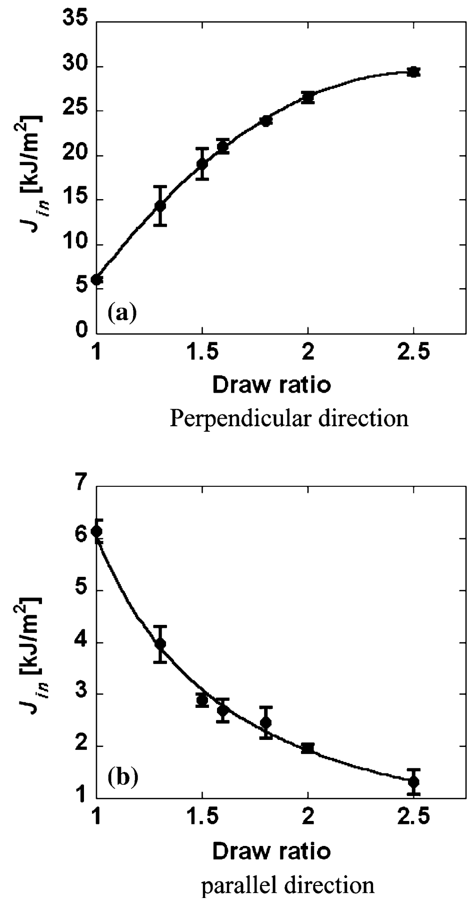

Fig. 1 Dependence of draw ratio on critical J-integral at crack initiation: (**a**) perpendicular direction (**b**) parallel direction

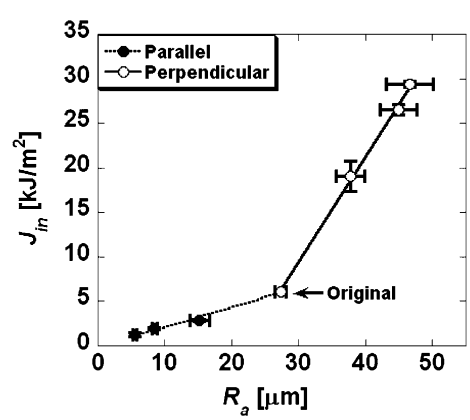

Fig. 2 Relationship between J_{in} and R_a

direction than in the parallel direction where such elongation and scission processes obviously decrease.

The relationship between J_{in} and R_a is shown in Fig. 2. It is clearly seen that the larger R_a value corresponds to the higher J_{in} value, indicating that the toughening mechanism in the parallel is considered to be accumulated damage generation in the crack-tip region that makes fracture surface much rougher.

SEM micrographs of fracture surfaces are shown in Fig. 3. The perpendicular with draw ratio 2.5 exhibited rougher surface with ductile deformation than the original. It is interesting to note that crevices existed on the fracture surfaces that were thought to be cracks transversely propagated between the parallel fibrils reoriented in the drawing direction. It is thus thought that the ductile deformation due to elongation of the oriented molecules and the transverse crack formation are primary mechanisms of toughening in draw-processed PLLA. On the other hand, the fracture surface of the parallel were much smoother than that of the original, corresponding to the lower J_{in} value.

J_{in} is contributed by energy dissipation through not only creation of fracture surface but also development of process zone. Damage formation in process zone can be analyzed by observing the notch-tip region using a POM. POM micrographs of notch-tip regions of the original and the perpendicular are shown in Fig. 4. In the original, multiple crazes forming a fan shape were observed. They were initiated from the initial notch-tip and propagated almost perpendicularly to the tensile direction. For the perpendicular with draw ratio 2.5, crazes were much denser and the width of the damage region was much wider than the original. Transverse cracks generated in the drawing direction are observed, and these obviously correspond to the crevices observed on the fracture surfaces as shown in Fig. 3b. Larger damage region consisting of crazes and transverse

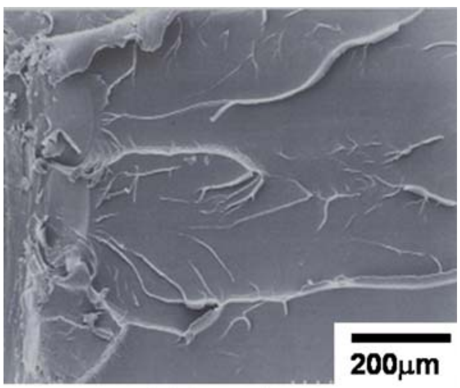

(a) draw ratio = 1

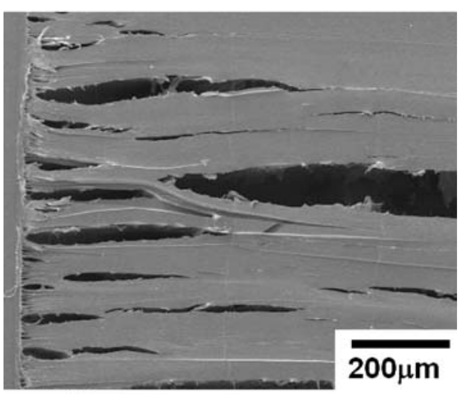

(b) draw ratio = 2.5, perpendicular

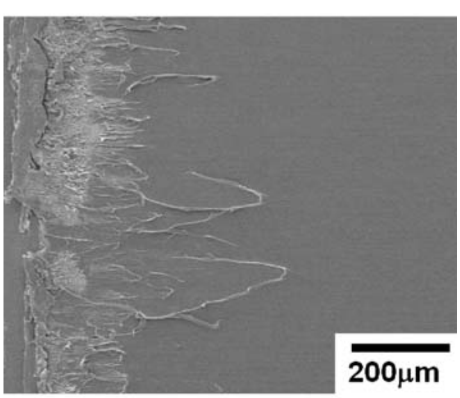

(c) draw ratio = 2.5, parallel

Fig. 3 SEM micrographs of fracture surfaces: (**a**) original (**b**) draw ratio = 2.5, perpendicular (**c**) draw ratio = 2.5, parallel

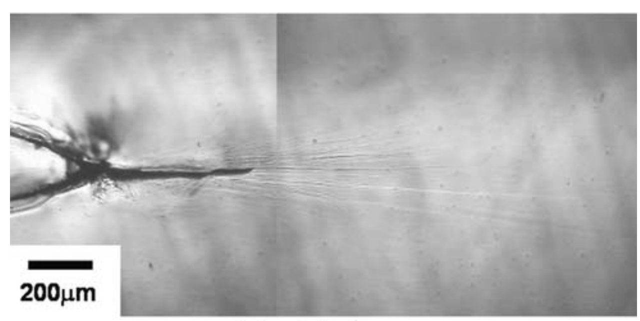

(a) original

(b) draw ratio = 2.5, perpendicular

Fig. 4 Polarizing optical microscope (POM) micrographs of damage zones: (**a**) original (**b**) draw ratio = 2.5, perpendicular cracks generated in crack-tip region indicates lager energy dissipation under crack initiation and propagation processes, and therefore, greater J_{in}.

In summary, the effect of drawing on the mode I fracture behavior of PLLA was investigated by evaluating the critical J-integral at crack initiation, J_{in}, and the surface roughness, R_a, and by performing SEM and POM of fracture mechanism. For the perpendicular direction, J_{in} increased as draw ratio increased; on the contrary, for the parallel direction, J_{in} decreased. The variation of R_a with draw ratio well coincided with that of J_{in}, suggesting that rough surface formation resulted in high energy dissipation during crack initiation. SEM and POM results indicated that the elongation and scission of the oriented molecules due to drawing, which usually create rough surface, are the primary mechanisms of the toughness improvement due to drawing.

References

1. Ikada Y, Shikinami Y, Hara Y, Tagawa M, Fukuda E (1996) J Biomed Mater Res 30:553
2. Tsuji H, Ikada Y (1995) Polymer 36:2709
3. Grizzi I, Garreau H, Li S, Vert M (1995) Biomaterials 16:305
4. Tsuji H, Ikada Y (1995) J Appl Polym Sci 58:1793
5. Suming L, McCarthy S (1999) Biomaterials 20:35
6. Todo M, Shinohara N, Arakawa K (2002) J Mater Sci Lett 21:1203
7. Todo M, Shinohara N, Arakawa K, Tsuji H (2003) Kobunshi Ronbunshu 60:644
8. Park SD, Todo M, Arakawa K (2004) J Mater Sci 39:1113
9. Park SD, Todo M, Arakawa K (2004) Key Eng Mater 261/263:105
10. Park SD, Todo M, Arakawa K (2005) J Mater Sci 40:1055
11. Park SD, Todo M, Arakawa K, Koganemaru M (2006) Polymer 47:1357
12. Uehara H, Yamazaki Y, Kanamoto T (1996) Polymer 37:57
13. Yamane A, Sawai D, Kameda T, Kanamoto T, Ito M, Porter RS (1997) Macromolecules 30:4170
14. Sawai D, Yamane A, Kameda T, Kanamoto T, Ito M, Yamazaki M, Hisatani K (1999) Macromolecules 32:5622
15. Mohanraj J, Chapleau N, Ajji A, Duckett RA, Ward IM (2003) J Appl Polym Sci 88:1336
16. Mohanraj J, Chapleau N, Ajji A, Duckett RA (2003) Polym Eng Sci 43:1317
17. Todo M, Takahashi K, Jar PYB, Beguelin Ph (1999) JSME Inter J 42:585
18. Todo M, Takahashi K, Beguelin Ph, Kausch HH (2000) Comp Sci Tech 60:763